Autonomous and Active Transport Operated by an Entropic DNA Piston

Bayoumi, Mariam; Nomidis, Stefanos K; Willems, Kherim; Carlon, Enrico; Maglia, Giovanni

[Link to publication in University of Groningen/UMCG research database](#)

NANO *LETTERS*

Letter

Autonomous and Active Transport Operated by an Entropic DNA Piston

Mariam Bayoumi, Stefanos K. Nomidis, Kherim Willems, Enrico Carlon,* and Giovanni Maglia*

Read Online

ACCESS | Metrics & More | Article Recommendations | Supporting Information

ABSTRACT: We present a synthetic nanoscale piston that uses chemical energy to perform molecular transport against an applied bias. Such a device comprises a 13 by 5 nm protein cylinder, embedded in a biological membrane enclosing a single-stranded DNA (ssDNA) rod. Hybridization with DNA cargo rigidifies the rod, allowing for transport of a selected DNA molecule across the nanopore. A strand displacement reaction from ssDNA fuel on the other side of the membrane then liberates the DNA cargo back into solution and regenerates the initial configuration. The entropic penalty of ssDNA confinement inside the nanopore drives DNA transport regardless of the applied bias. Multiple automated and reciprocating cycles are observed, in which the DNA piston moves through the 10 nm length of the nanopore. In every cycle, a single DNA molecule is transported across the nanopore against an external bias force, which is the hallmark of biological transporters.

KEYWORDS: nanotransport, synthetic device, DNA nanotechnology, molecular transport, nanomachine
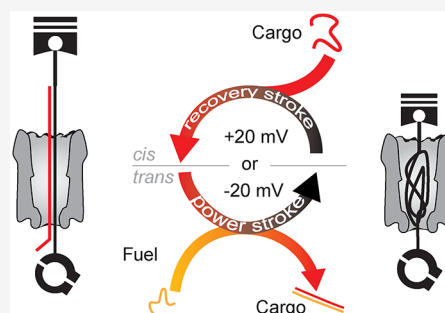
INTRODUCTION

Biological molecular devices have long been a constant source of inspiration for scientists, and much effort has been devoted to building molecular machines that mimic their natural counterpart,[1−4] or to adding new functions in existing biological systems.[5] Another interesting area of research is the reproduction of macroscopic functions at the nanoscale.[6,7] Initial efforts to reproduce machine-like behavior with synthetic systems focused on using organic chemistry to make interlocked systems, such as rotaxanes (dumbbell-shaped molecules, threaded through macrocycles), which are crucial elements of many biological machines, including ATP synthases and bacterial flagellar motors. Synthetic interlocked systems have been made to work as molecular shuttles, where multiple states are stochastically sampled, or molecular switches, where interconversion between states is controlled by applying an external stimulus.[8] Artificial interlocked systems with remarkable machine-like behaviors have also been described.[9−11] Applying these, and other synthetic principles, complex molecular machines have been prepared that undergo translational motions or rotations operated upon by external stimuli such as light, pH change or oxidation/reduction.[12,13] However, an important characteristic of a biological molecular machine is its ability of using chemical fuels to autonomously and repeatedly cycle through asymmetric nanomechanical states while continuously transducing potential chemical energy into work, as long as the fuel is present.[8] And, making such synthetic systems has proven more challenging.

The introduction of autonomous actuation and reciprocation in a synthetic machine will most likely require switching to softer and larger nanostructures, such as those made by biological polymers. This is because, compared to small organic molecules, polymers allow building larger nanomachines, which can deal better with design complexity. Moreover, nanostructures made by several soft interactions allow a more efficient dissipation of the thermal energy, which is one of the main challenges when building at the nanoscale. Nucleic acids are emerging as an ideal building material in nanotechnology, because their self-assembly can be programmed by following the predictability of Watson–Crick interactions; moreover, strand displacement reactions allow the remodeling of the energy landscape of DNA nanostructures. The list of achievements using DNA nanomachines include programmable walkers[14,15] and molecular synthesizers.[16] Such systems can perform autonomous and isothermal operations; however, they differ from biological machines, as they have only been shown to operate in one cycle.

Synthetic transmembrane devices that combine the modularity of DNA nanotechnology with the precise engineering and chemical diversity of natural proteins have been designed. Examples include a protein nanopore decorated with DNA arms, that facilitated the passive transport a DNA cargo across a membrane using single-stranded DNA (ssDNA) as fuel,[17] a nanopore that moved a DNA-PEG thread with the combined
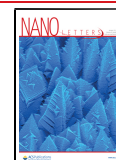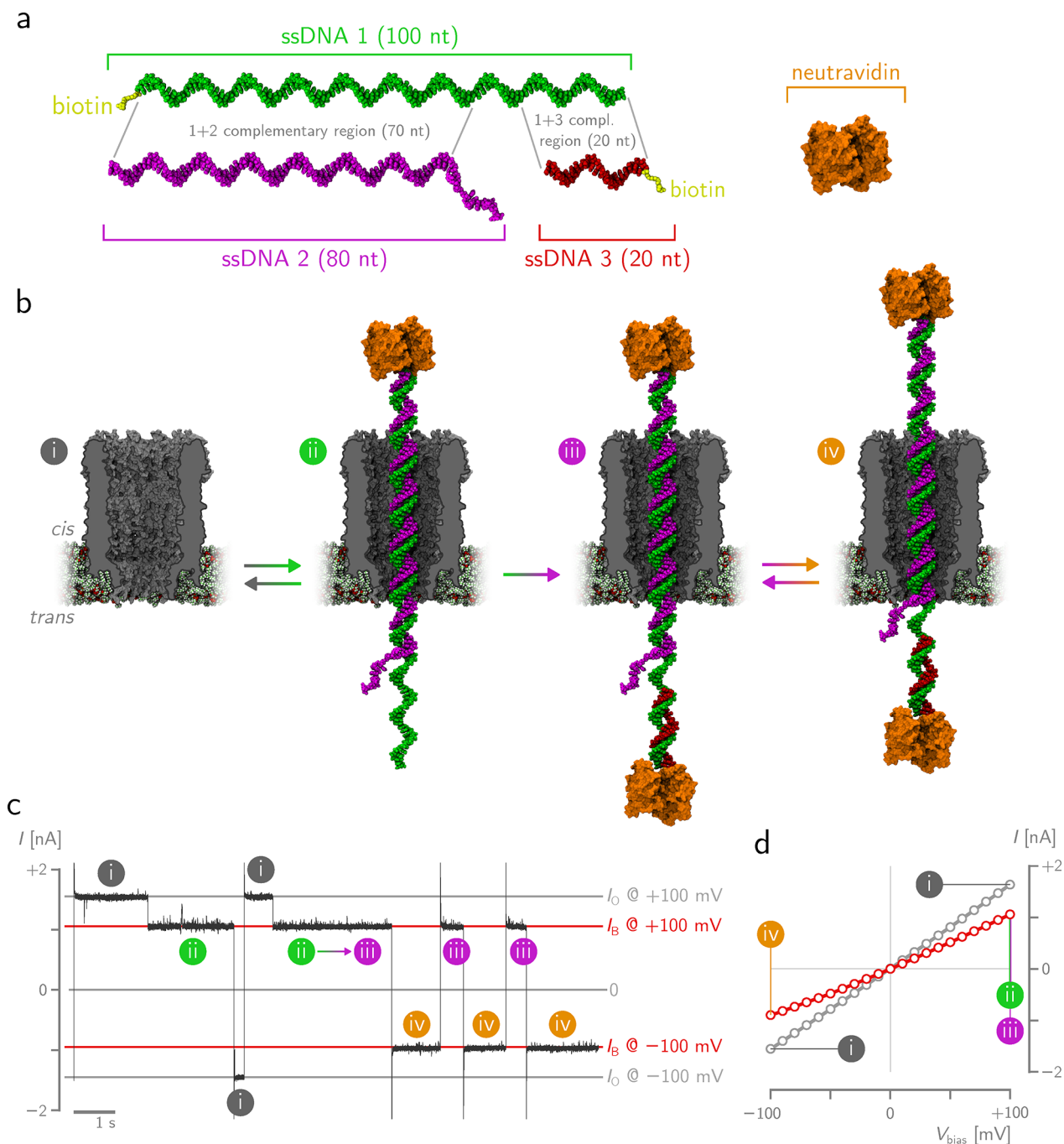
Figure 1. Rotaxane formation. (a) Molecular components of rotaxane-ds: ssDNA (**ssDNA 1**, green, and **ssDNA 2**, purple, in cis; and **ssDNA 3**, red, in trans) and neutravidin (**NA**, cis and trans, orange) molecules are used to form the rotaxane. (b) Atomistic representation and (c) current trace of rotaxane assembly inside ClyA. From the open pore (i) at positive voltage, the **ssDNA 1/ssDNA 2/NA** complex remains trapped in pore (ii). By reversing the voltage, the system returns to the open-pore state (i). When **NA** and **ssDNA 3** are added to the trans side at positive voltage, hybridization with the **ssDNA 1** overhang leads to the formation of rotaxane-ds (iii). This is permanently trapped in the nanopore, as revealed by inverting the voltage (iv). The horizontal gray and red lines underneath the current traces correspond to the open-pore and blocked currents, respectively, measured at +100 mV and −100 mV, proving the formation of the rotaxane. (d) I−V plots for the open pore (gray) and rotaxane-ds (red). The electrical recordings were carried out in 2 M NaCl, 15 mM Tris-HCl, pH 7.5 at 22 °C. Data were recorded by applying a 10 kHz low-pass Bessel filter, and using a 20 μs (50 kHz) sampling rate. Images were rendered using VMD.[38]

action of an ATP-powered DNA polymerase and a strand displacement reaction,[18] and a molecular hopper that could directionally move DNA cargos in an electric field.[19] However, despite the fact that a reciprocating nanoscale motion was achieved, the transmembrane bias was crucial to dictate the direction and molecular actuation.

In this work, we have built a fully synthetic nanoscale device that uses the free energy of DNA hybridization through strand displacement to actively transport a DNA molecule across a membrane against a transmembrane potential. To the best of our knowledge this is the first synthetic device with such characteristics. Insights about the underlying operating principle are obtained from molecular dynamics simulations, which
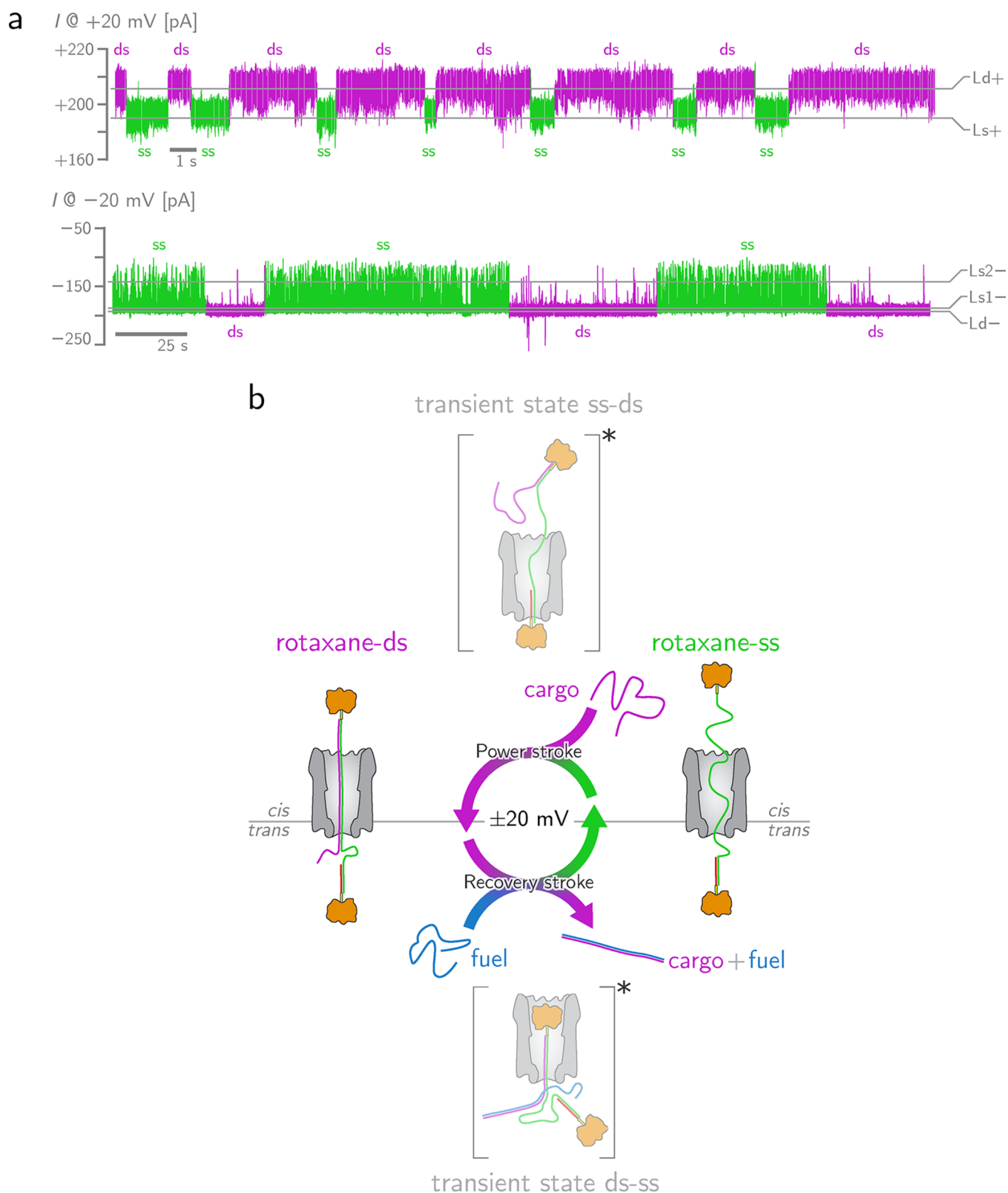
Figure 2. Entropic piston cycles. (a) Current traces showing the nanopiston cycling between the rotaxane-ds (purple) and rotaxane-ss (green) conformations, under a constant bias of −20 mV (top) and −20 mV (bottom) bias. The transition is induced through hybridization with the fuel and cargo in the trans and cis chambers. The gray horizontal lines indicate the average currents in rotaxane-ds and rotaxane-ss, labeled with Ld and Ls, respectively. Note that, the analysis of the rotaxane-ss current at −20 mV reveals two sublevels, Ls1 and Ls2 (see Section S6). (b) Schematic representation of the proposed states involved in a full cycle. The top and bottom states are the likely short-lived intermediate states (indicated by an asterisk). The electrical recordings were carried out at +20 mV in 2 M NaCl, 15 mM Tris-HCl, pH 7.5 at 22 °C. Data were recorded by applying a 2 kHz low-pass Bessel filter, using a 100 μs (10 kHz) sampling rate.

Figure 3. Center: Representative conformations obtained from coarse-grained simulations of rotaxane-ds (left) and -ss (right) at zero bias (for model details see Section S4). The color coding follows that of Figures 1 and 2: dsDNA is represented as a sequence of beads with alternating green and purple beads, matching those of the two constituent strands. Side graphs: Histograms indicating the position (see eq S1) of the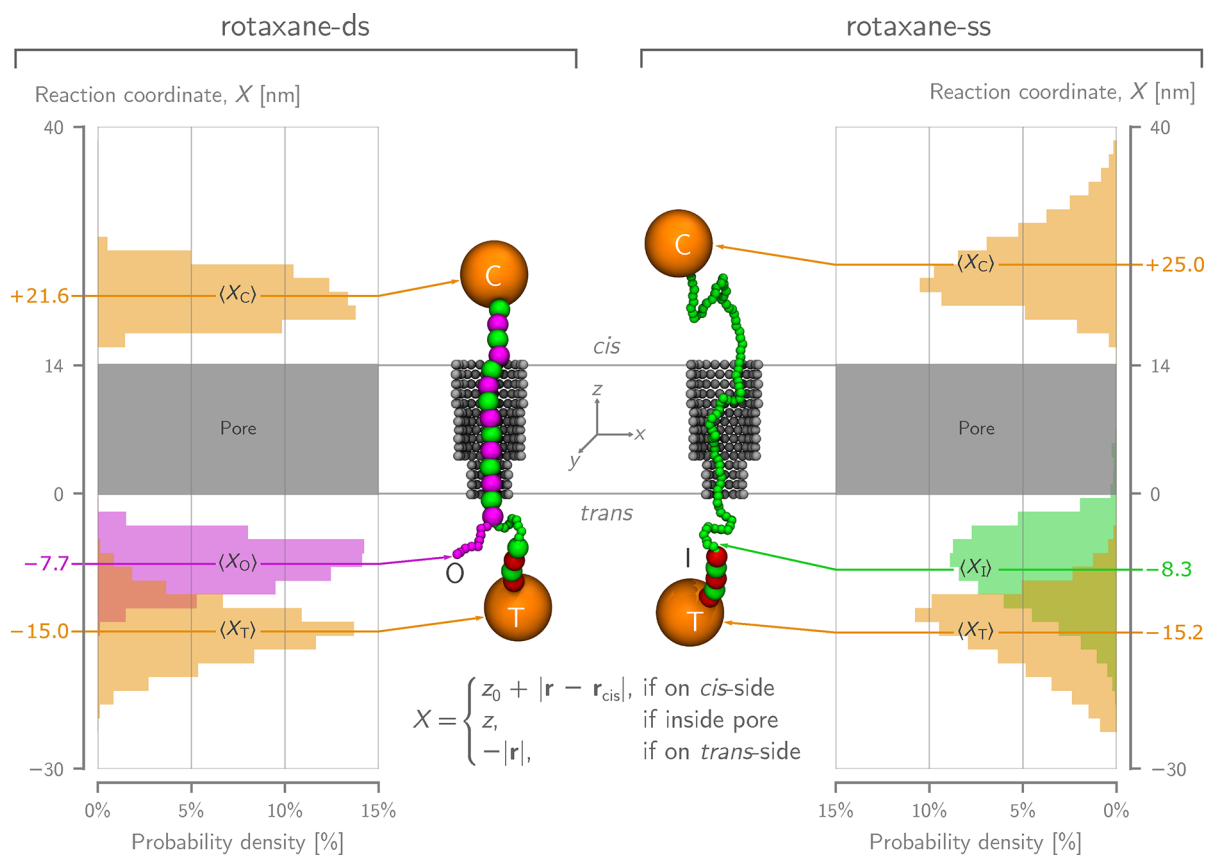 two neutravidins (C and T, orange), together with the ssDNA overhang (O, purple) and ssDNA/dsDNA interface (I, green), for rotaxane-ds (left) and rotaxane-ss (right). The average values of these positions are indicated by the colored horizontal lines. The simulations indicate that the ssDNA overhang in rotaxane-ss and ssDNA/dsDNA interface in rotaxane-ds are exposed to the trans solutions. Images were rendered using VMD.[38]

suggest that the piston takes advantage of the entropic difference between the nanoscale confinement of ssDNA and double-stranded DNA (dsDNA) inside the nanopore. This device can perform several reciprocating cycles of actuation, and can transport DNA against the applied potential, hence truly operating as a natural molecular machine.

■ RESULTS

The main building block of the nanopiston is the bacterial transmembrane protein Cytolysin A (ClyA).[20,21] Here we use ClyA-AS[22] a modified version engineered for nanopore analysis.[23−31] The *lumen* of ClyA (5.5 nm diameter) and narrower constriction (3.3 nm diameter, Figure 1) allow the entry and translocation of dsDNA under an applied potential.[17,32] By contrast, ssDNA cannot efficiently enter the nanopore,[17,32] an effect most likely due to the high entropic energy required to confine ssDNA inside the nanopore.[33] We constructed rotaxanes using a DNA thread interposed between two neutravidin stoppers, which was trapped within a ClyA nanopore. The rotaxane is built from three ssDNA sequences: **ssDNA 1**, **ssDNA 2**, and **ssDNA 3** and two neutravidin stoppers (Figure 1a, b). Neutravidin (0.5 μM), **ssDNA 1** (5′-biotinylated, 100 bases, 1.2 μM) and **ssDNA 2** (80 bases, 1 μM) were added to the cis solution. The last 70 bases of **ssDNA 2** are complementary to the first 70 bases of **ssDNA 1** (Table S1), hence a complex with neutravidin on one end, a 70-base dsDNA and two ssDNA overhangs on the other end is formed. This

complex is captured by the nanopore at +100 mV (where a positive applied potential drives the DNA from the cis toward the trans side) and remains trapped indefinitely, until the potential is reversed and the open-pore current restored (Figure 1c). While keeping the potential at +100 mV, the addition to the trans side of neutravidin (1 μM) and **ssDNA 3** (3′-biotinylated, 20 bases, 2 μM), complementary to the last ten bases of the **ssDNA 1** overhang of the trapped thread, completes the rotaxane by hybridization. We refer to this complex as rotaxane-ds, as it is predominantly formed by dsDNA, with a short flexible ssDNA connection and an ssDNA overhang. By reversing the potential after the formation of rotaxane-ds, the open-pore current cannot be recovered, indicating that rotaxane-ds is permanently trapped within the pore (Figure 1c). Both open pore and rotaxane-ds have linear current—voltage (*IV*) relationships in the range ±100 mV (Figure 1d), from the slope of which the nanopore conductance can be calculated: 14.3 ± 0.6 nS for the open pore and 9.39 ± 0.68 nS for rotaxane-ds as the DNA inside the pore reduces the ionic flow through it.

Once rotaxane-ds is formed, the addition of **ssDNA 4** (0.5 μM) to the trans chamber, which is fully complementary to **ssDNA 2**, induces the displacement of the latter in trans via a strand displacement reaction, using the **ssDNA 2** overhang as a toehold (Figure 2). During the strand displacement reaction, the cis neutravidin is transiently pushed toward the trans side, most likely entering the lumen of the nanopore (see Section S3). Indeed, previous studies have shown that avidin can enter the cis

lumen of ClyA but cannot translocate through the nanopore.[34] After the removal of **ssDNA 2**, a new configuration is obtained, in which **ssDNA 1** and **ssDNA 3** remain trapped within the pore. This configuration consists of a 90-base-ssDNA thread on the cis end, a 10-basepair-dsDNA stretch on the trans side, and neutravidin on both sides of the pore (Figure 2). We refer to this configuration as rotaxane-ss. When **ssDNA 4b**, a ssDNA molecule that is only complementary to the first 60 bases of **ssDNA 2,** was added to the trans side, rotaxane-ss could not form (Figure S1), indicating that a strand reaction is required to transition from rotaxane-ds to rotaxane-ss.

The ionic current of rotaxane-ss (I_{res} = 64.5 ± 0.6% at +20 mV) is lower than the blocked current of rotaxane-ds (I_{res} = 68.4 ± 0.5% at +20 mV, Figure 2a), most likely reflecting the coiled structure of ssDNA inside the nanopore (Figure 2). When **ssDNA 4** fuel alone is added to the trans chamber, a single strand displacement reaction with **ssDNA2** takes place, and the system remains in the rotaxane-ss state indefinitely (Figure 2a and Figure S2). Similar states are observed at −20 mV, although the current blockades were slightly different (I_{res} = 64.0 ± 1.5% and 66.8 ± 0.4% for rotaxane-ss and rotaxane-ds, respectively), reflecting the asymmetric structure of the two rotaxanes (Figure 2e, see the Supporting Information). The subsequent addition of 0.5 μM **of ssDNA 2** cargo to the cis side restores rotaxane-ds, as **ssDNA 2** hybridizes with the thread of rotaxane-ss. Under multiple turnover conditions (i.e., 0.5 μM of **ssDNA 4** fuel in trans and 0.5 μM of **ssDNA 2** cargo in cis) several current cycles were observed, corresponding to the swapping between the two rotaxanes: ds → ss → ds → ss →··· These cycles were found to be both at positive, + 20 mV (Figure 2a, top trace), + 50 mV and +100 mV (Figure S3), and negative, − 20 mV (Figure 2a, bottom trace), biases. Higher negative applied potentials (e.g., −50 mV, Figure S3) prevented the cycling. Furthermore, the cycles were faster at positive than at negative applied potentials, but were slower as the potential was increased. This voltage dependency can be explained by toehold sequestering inside the nanopore (Section S2 for a kinetic and mechanistic description of the cycles). After each cycle, one cargo molecule is transported from cis to trans and one fuel molecule is expended (Figure 2).

We performed a series of coarse-grained molecular dynamics simulations to investigate the typical conformations of rotaxanes-ds and ss at zero bias. This approach is justified by the long time scales of interest, and the high salt concentration of the solution (2 M KCl). A numerical analysis of the electrostatic energies, using the Poisson−Boltzmann equations, indeed indicates that electrostatic DNA-nanopore interactions are weak and repulsive (Figures S4 and S5 in Section S8). These interactions were accounted for by properly adjusting the dimensions of the pore (Figure S6). Moreover, the fact that the piston operates at both positive and negative applied bias suggests that the electrophoretic bias is not necessary for its functioning. Indeed, simulations indicate that entropy plays a more central role. Rotaxane-ds has two, 10-base-long, ssDNA fragments. One is the 5′ overhang that is used as toehold for the strand displacement reaction, the other is the ssDNA connecting the two rigid dsDNA fragments (Figure 3a). Simulations show that, even at zero bias, entropic forces push rotaxane-ds toward the trans chamber, with the cis neutravidin remaining, on average, at a distance of 5 nm from the pore entry (Figure 3). The hinge and toehold stay outside of the trans pore entry because positioning of the flexible hinge inside the pore would greatly suppress the conformational fluctuations of the molecule.

Under these conditions, the toehold is accessible for the strand displacement reaction. Rotaxane-ss shows larger conformational fluctuations, because of its long flexible ssDNA part. Nonetheless, the simulations indicate that the dsDNA segment remains outside of the nanopore on the trans side. At the same time, the ssDNA end of rotaxane-ss stretches out toward the cis side (Figure 3) and is accessible for hybridization with **ssDNA 2**. Thus, during the formation of the rotaxane-ds, the entropic penalty of keeping two ssDNA stretches inside the nanopore drives the transport of the **ssDNA 2** toehold toward the trans side, even against an applied potential. Then a strand displacement reaction reforms rotaxane-ss, which leads to a second entropy-driven shift that pushes the ssDNA thread toward the cis side (i.e., an upward displacement of the piston, see Movie S1). The crucial role of entropy has also been demonstrated in another class of rotaxanes, composed of dsDNA and ssDNA of varying lengths (see Section S7 and Movie S2).

■ CONCLUSION

Many transmembrane biological systems use an interlocked architecture and channel the free energy of a chemical gradient to power molecular motion or to transport molecules. For example, the bacterial flagella motor and the F_1F_0 rotary ATP synthase rotary motor possess a transmembrane rotaxane-like architecture that convert a transmembrane proton gradient into unidirectional motion[35] or to synthesize ATP,[36] respectively. Here, we describe a molecular device made of a DNA-neutravidin piston enclosed into a protein nanopore cylinder, which is based upon a new operating principle. A strand displacement reaction induces a power stroke, which moves the piston ~10 nm in the cis-to-trans direction (Figure 2). This leaves the rotaxane at a low-entropy state, which provides a recovery stroke to move the piston back to the cis solution. The hybridization with a ssDNA strand in solution recovers the initial configuration (Figure 2). Hence, unidirectional molecular motion is obtained by focusing the free energy of DNA hybridization inside the nanopore cylinder and by exploiting the different entropy of nanoscale confinement. During each cycle of the nanopiston, a ssDNA molecule is transported from the cis to the trans compartment through the nanopore. This device can operate at positive and negative applied potentials, indicating that the free energy of DNA hybridization allows moving DNA against an external bias force, which is the hallmark of biological active transporters.

■ METHODS

All DNA was purchased from Integrated DNA Technologies (IDT). Double-stranded DNA was formed by incubation of the complementary strands at 95 °C for 1 h and then letting it cool down overnight. ClyA nanopores were expressed and purified, as described in detail before.[22]

Single-Channel Recording. A planar lipid bilayer was formed with DPhPC (1,2-diphytanoyl-*sn*-glycero-3-phospho-choline) lipids across two chambers filled with buffer (2 M NaCl, 15 mM Tris-HCl, pH 7.5). A detailed explanation of this technique and the equipment used in this work has been described before.[37] Next, 0.01−0.1 ng mL^{-1} of the ClyA oligomers were added to the electrophysiology chamber to obtain single channels. The signal was collected at a sampling rate of 50 kHz after processing with a 10 kHz Bessel filter. The

length of each step of the cycle was collected manually and expressed as the median values ± the standard error of the mean.

■ ASSOCIATED CONTENT

Ⓢ Supporting Information

The Supporting Information is available free of charge at https://pubs.acs.org/doi/10.1021/acs.nanolett.0c04464.

List of the DNA sequences used in this work, a detailed explanation of the nanopiston cycles including a table of free energy of DNA hybridization, an explanation of the transient states during the cycling, a physical analysis of the current fluctuations, additional experiments with mixed rotaxanes, and additional figures (PDF)

Movie S1, showing the states of rotaxane-ds and rotaxane-ss before and after a strand displacement reaction (MP4)

Movie S2, demonstrating the crucial role of entropy in another class of rotaxanes composed of dsDNA and ssDNA of varying lengths (MP4)

■ AUTHOR INFORMATION

Corresponding Authors

Enrico Carlon − *KU Leuven, Soft Matter and Biophysics Unit, Department of Physics and Astronomy, 3001 Leuven, Belgium;* Ⓞ orcid.org/0000-0001-8266-1096; Email: enrico.carlon@kuleuven.be

Giovanni Maglia − *Groningen Biomolecular Sciences & Biotechnology Institute, University of Groningen, Groningen 9747 AG, The Netherlands; Department of Chemistry, KU Leuven, Leuven 3001, Belgium;* Ⓞ orcid.org/0000-0003-2784-0811; Email: g.maglia@rug.nl

Authors

Mariam Bayoumi − *Department of Chemistry, KU Leuven, Leuven 3001, Belgium; Center for Brain & Disease Research, VIB-KU Leuven, Leuven 3000, Belgium*

Stefanos K. Nomidis − *KU Leuven, Soft Matter and Biophysics Unit, Department of Physics and Astronomy, 3001 Leuven, Belgium; Flemish Institute for Technological Research (VITO), Mol B-2400, Belgium*

Kherim Willems − *imec, Leuven 3001, Belgium;* Ⓞ orcid.org/0000-0003-1341-1581

Complete contact information is available at:
https://pubs.acs.org/10.1021/acs.nanolett.0c04464

Notes

The authors declare no competing financial interest.

■ ACKNOWLEDGMENTS

■ REFERENCES

(1) Watson, M. A.; Cockroft, S. L. Man-Made Molecular Machines: Membrane Bound. *Chem. Soc. Rev.* **2016**, *45* (22), 6118−6129.

(2) Langecker, M.; Arnaut, V.; Martin, T. G.; List, J.; Renner, S.; Mayer, M.; Dietz, H.; Simmel, F. C. Synthetic Lipid Membrane Channels Formed by Designed DNA Nanostructures. *Science (Washington, DC, U. S.)* **2012**, *338* (6109), 932−936.

(3) Bell, N. A.; Engst, C. R.; Ablay, M.; Divitini, G.; Ducati, C.; Liedl, T.; Keyser, U. F. DNA Origami Nanopores. *Nano Lett.* **2012**, *12* (1), 512−517.

(4) Burns, J. R.; Stulz, E.; Howorka, S. Self-Assembled DNA Nanopores That Span Lipid Bilayers. *Nano Lett.* **2013**, *13* (6), 2351−2356.

(5) Ho, C.-W.; Van Meervelt, V.; Tsai, K.-C.; De Temmerman, P.-J.; Mast, J.; Maglia, G. Engineering a Nanopore with Co-Chaperonin Function. *Sci. Adv.* **2015**, *1* (11), No. e1500905.

(6) Kudernac, T.; Ruangsupapichat, N.; Parschau, M.; Macia, B.; Katsonis, N.; Harutyunyan, S. R.; Ernst, K. H.; Feringa, B. L. Electrically Driven Directional Motion of a Four-Wheeled Molecule on a Metal Surface. *Nature* **2011**, *479* (7372), 208−211.

(7) Lancia, F.; Ryabchun, A.; Katsonis, N. Life-like Motion Driven by Artificial Molecular Machines. *Nat. Rev. Chem.* **2019**, *3* (9), 536−551.

(8) Watson, M. A.; Cockroft, S. L. Man-Made Molecular Machines: Membrane Bound. *Chem. Soc. Rev.* **2016**, *45*, 6118.

(9) Huang, T. J.; Brough, B.; Ho, C.-M.; Liu, Y.; Flood, A. H.; Bonvallet, P. A.; Tseng, H.-R.; Stoddart, J. F.; Baller, M.; Magonov, S. A Nanomechanical Device Based on Linear Molecular Motors. *Appl. Phys. Lett.* **2004**, *85* (22), 5391−5393.

(10) Lewandowski, B.; De Bo, G.; Ward, J. W.; Papmeyer, M.; Kuschel, S.; Aldegunde, M. J.; Gramlich, P. M. E.; Heckmann, D.; Goldup, S. M.; D'Souza, D. M.; Fernandes, A. E.; Leigh, D. A. Sequence-Specific Peptide Synthesis by an Artificial Small-Molecule Machine. *Science (Washington, DC, U. S.)* **2013**, *339* (6116), 189−193.

(11) Cheng, C.; McGonigal, P. R.; Schneebeli, S. T.; Li, H.; Vermeulen, N. A.; Ke, C.; Stoddart, J. F. An Artificial Molecular Pump. *Nat. Nanotechnol.* **2015**, *10* (6), 547−553.

(12) Badjić, J. D.; Balzani, V.; Credi, A.; Silvi, S.; Stoddart, J. F.; Badjic, J. D.; Balzani, V.; Credi, A.; Silvi, S.; Stoddart, J. F. A Molecular Elevator. *Science (Washington, DC, U. S.)* **2004**, *303* (5665), 1845−1849.

(13) Champin, B.; Mobian, P.; Sauvage, J.-P. Transition Metal Complexes as Molecular Machine Prototypes. *Chem. Soc. Rev.* **2007**, *36* (2), 358−366.

(14) Omabegho, T.; Sha, R.; Seeman, N. C. A Bipedal DNA Brownian Motor with Coordinated Legs. *Science (Washington, DC, U. S.)* **2009**, *324* (5923), 67−71.

(15) Shin, J.-S.; Pierce, N. A. A Synthetic DNA Walker for Molecular Transport. *J. Am. Chem. Soc.* **2004**, *126* (35), 10834−10835.

(16) He, Y.; Liu, D. R. Autonomous Multistep Organic Synthesis in a Single Isothermal Solution Mediated by a DNA Walker. *Nat. Nanotechnol.* **2010**, *5* (11), 778−782.

(17) Franceschini, L.; Soskine, M.; Biesemans, A.; Maglia, G. A Nanopore Machine Promotes the Vectorial Transport of DNA across Membranes. *Nat. Commun.* **2013**, *4*, 2415.

(18) Watson, M. A.; Cockroft, S. L. An Autonomously Reciprocating Transmembrane Nanoactuator. *Angew. Chem., Int. Ed.* **2016**, *55* (4), 1345−1349.

(19) Qing, Y.; Ionescu, S. A.; Pulcu, G. S.; Bayley, H. Directional Control of a Processive Molecular Hopper. *Science (Washington, DC, U. S.)* **2018**, *361* (6405), 908−912.

(20) von Rhein, C.; Bauer, S.; Lopez Sanjurjo, E. J.; Benz, R.; Goebel, W.; Ludwig, A. ClyA Cytolysin from Salmonella: Distribution within the Genus, Regulation of Expression by SlyA, and Pore-Forming Characteristics. *Int. J. Med. Microbiol.* **2009**, *299* (1), 21−35.

(21) Soskine, M.; Biesemans, A.; Moeyaert, B.; Cheley, S.; Bayley, H.; Maglia, G. An Engineered ClyA Nanopore Detects Folded Target Proteins by Selective External Association and Pore Entry. *Nano Lett.* **2012**, *12* (9), 4895−4900.

(22) Soskine, M.; Biesemans, A.; De Maeyer, M.; Maglia, G. Tuning the Size and Properties of ClyA Nanopores Assisted by Directed Evolution. *J. Am. Chem. Soc.* **2013**, *135* (36), 13456−13463.

(23) Biesemans, A.; Soskine, M.; Maglia, G. A Protein Rotaxane Controls the Trans Location of Proteins Across a ClyA Nanopore. *Nano Lett.* **2015**, *15* (9), 6076−6081.

(24) Wloka, C.; Van Meervelt, V.; van Gelder, D.; Danda, N.; Jager, N.; Williams, C. P.; Maglia, G. Label-Free and Real-Time Detection of Protein Ubiquitination with a Biological Nanopore. *ACS Nano* **2017**, *11* (5), 4387−4394.

(25) Van Meervelt, V.; Soskine, M.; Maglia, G. Detection of Two Isomeric Binding Configurations in a Protein-Aptamer Complex with a Biological Nanopore. *ACS Nano* **2014**, *8* (12), 12826−12835.

(26) Willems, K.; Van Meervelt, V.; Wloka, C.; Maglia, G. Single-Molecule Nanopore Enzymology. *Philos. Trans. R. Soc., B* **2017**, *372* (1726), 20160230.

(27) Zernia, S.; van der Heide, N. J.; Galenkamp, N. S.; Gouridis, G.; Maglia, G. Current Blockades of Proteins inside Nanopores for Real-Time Metabolome Analysis. *ACS Nano* **2020**, *14* (2), 2296−2307.

(28) Soskine, M.; Biesemans, A.; Maglia, G. Single-Molecule Analyte Recognition with ClyA Nanopores Equipped with Internal Protein Adaptors. *J. Am. Chem. Soc.* **2015**, *137* (17), 5793−5797.

(29) Willems, K.; Ruic, D.; L. R. Lucas, F.; Barman, U.; Verellen, N.; Hofkens, J.; Maglia, G.; Van Dorpe, P. Accurate Modeling of a Biological Nanopore with an Extended Continuum Framework. *Nanoscale* **2020**, *12* (32), 16775−16795.

(30) Van Meervelt, V.; Soskine, M.; Singh, S.; Schuurman-Wolters, G. K.; Wijma, H. J.; Poolman, B.; Maglia, G. Real-Time Conformational Changes and Controlled Orientation of Native Proteins Inside a Protein Nanoreactor. *J. Am. Chem. Soc.* **2017**, *139* (51), 18640−18646.

(31) Galenkamp, N. S.; Soskine, M.; Hermans, J.; Wloka, C.; Maglia, G. Direct Electrical Quantification of Glucose and Asparagine from Bodily Fluids Using Nanopores. *Nat. Commun.* **2018**, *9* (1), 4085.

(32) Franceschini, L.; Brouns, T.; Willems, K.; Carlon, E.; Maglia, G. DNA Translocation through Nanopores at Physiological Ionic Strengths Requires Precise Nanoscale Engineering. *ACS Nano* **2016**, *10* (9), 8394−8402.

(33) Nomidis, S. K.; Hooyberghs, J.; Maglia, G.; Carlon, E. DNA Capture into the ClyA Nanopore: Diffusion-Limited versus Reaction-Limited Processes. *J. Phys.: Condens. Matter* **2018**, *30* (30), 304001.

(34) Lu, B.; Stokes, C.; Fahie, M.; Chen, M.; Golovchenko, J. A.; Hau, L. V. Protein Motion and Configurations in a Form-Fitting Nanopore: Avidin in ClyA. *Biophys. J.* **2018**, *115* (5), 801−808.

(35) Sowa, Y.; Berry, R. M. Bacterial Flagellar Motor. *Q. Rev. Biophys.* **2008**, *41* (2), 103−132.

(36) Kühlbrandt, W. Structure and Mechanisms of F-Type ATP Synthases. *Annu. Rev. Biochem.* **2019**, *88* (1), 515−549.

(37) Maglia, G.; Heron, A. J. J. A. J.; Stoddart, D.; Japrung, D.; Bayley, H. Analysis of Single Nucleic Acid Molecules with Protein Nanopores. *Methods Enzymol.* **2010**, *475* (C), 591−623.

(38) Humphrey, W.; Dalke, A.; Schulten, K. VMD: Visual Molecular Dynamics. *J. Mol. Graphics* **1996**, *14* (1), 33−38.